Available online at www.sciencedirect.com

ScienceDirect

Procedia Manufacturing 35 (2019) 223–228

Procedia MANUFACTURING

www.elsevier.com/locate/procedia

2nd International Conference on Sustainable Materials Processing and Manufacturing

(SMPM 2019)

The Fluid Flow Effect on the Inlet Injection of the Thin Film Deposition in a Square Type Atomic Layer Deposition Reactor

Rigardt Alfred Maarten Coetzee[a]*, Hong-Liang Lu[b], Tien-Chien Jen[a]

[a] *University of Johannesburg, Aukland Park, Johannesburg 2006, South Africa*
[a] *State Key Laboratory of ASIC and Systems, Shanghai Institute of Intelligent Electronics & Systems, Fudan University, Shanghai 200433, China*

Abstract

In recent years, industry is ever striving to deposit optimal thin films on nano devices. This strive led to interest in utilizing advance nano-manufacturing techniques that can fabricate ever-decreasing scale products along with films that provide highly uniform, conformal, and pin-hole-free quality thin films. Atomic layer deposition provides a technique that fulfil these requirements. However, the understanding of the deposition process within the fabrication of these thin films are still greatly not well-known. The fluid flow patterns and distributions within the atomic layer deposition reactors are rarely investigated and lacks the fluid flow effect incorporated along with the deposition process near the substrate. Per se, these effects due to the geometrical effect of the inlet injection location from the deposited substrate of a square type Gemstar Reactor is investigated. The findings reveal the inlet flow effect, near substrate flow behavior, and optimal selection for the deposition of aluminium oxide (Al_2O_3) thin film. The study simulates the fluid flow properties along with the chemical kinetics by applying computational fluid dynamics incorporated within ANSYS Fluent Software. The flow and surface reaction of Trimethylaluminium and Ozone as precursors, and Argon as the purging gas, are incorporated within the atomic layer deposition sequence. The findings reveal close similarities to that of previous literature.

Peer-review under responsibility of the organizing committee of SMPM 2019.

* Corresponding author. Tel.: +27-76-500-8904.
E-mail address: rcoetzee@uj.ac.za

2351-9789
Peer-review under responsibility of the organizing committee of SMPM 2019.
10.1016/j.promfg.2019.06.002

Keywords: Nanotechnology; atomic layer deposition; computational fluid dynamics; backward facing step flow; thin film

1. Introduction

In the modern Nano-manufacturing process, precision and absolute control is of necessity to further the capability and continual size shrinkage of cutting-edge technologies. A Nano-manufacturing technique called atomic layer deposition (ALD) has introduced a key-enabling nanotechnology process that is capable of producing superior ultrathin, uniform, conformal and pinhole-free Nano-films on complex topography, above its predecessors [1, 2]. These attributes made ALD a favorable deposition-technique to produce a variety of ultra-thin films for cutting edge fuel cells, solar cells, microelectronics, superconductors, and medical equipment, among other applications [3]. The deposition process of ALD is based on dividing the process into self-limiting surface reactions concerning the gaseous precursors, and the absorbed species on the substrate [2]. The procedure involves four repetitive sequential steps: Firstly, by exposing and saturating the substrate surface to the first precursor by the first pulse; then after, purging the excess precursor and volatile by-products from the reactor; the saturated substrate layer is then introduced to react with the second precursor; and once again the volatile by-products and excess are purged from the reactor. These steps are illustrated schematically in Figure 1 (A). These self-limiting repetitive saturated steps, ensures a layer-by-layer control over growing thin film [2]. Generally, in recent years, the ALD process that consists of a multi-scale process was studied either experimental or numerically. Experimental studies being more favorable than the latter, none the less, the computational simulation models assist researchers in unveiling the underlining atomic layer deposition process. This is done to comprehend and predict the effects of parameters on both process characteristics and final thin film product properties [4-6]. Due to the complexity and challenges this technique presents from its dependency on the behavioural nature of the reactants and in the process operating conditions, research remains scarce and ongoing. A common and interesting phenomenon that has been revealed to be of interest within ALD reactors, but scarcely been observed for ALD application, is that of flow separation due to sudden flow expansion. This phenomenon is popularly known in fluid mechanics as the Backward-Facing Step flow (BFS) [7]. The BFS has been the focus of intensive study for many years. Typically, BFS studies in two-dimensional (2D) and three-dimensional (3D) is popular with a classical set of simple geometric configurations, such as a flow of a channel with a sudden step expansion. In the past decades, simulation attempts include the study of the flow patterns at numerous Reynolds number and flow states [8], heat and mass transfer effects [9], homogenous combustion reaction [10], as well as micro-step and Nano-fluid flow characteristics [11]. The BFS phenomenon consist of complex flow pattern and regions downstream of a backward-facing step, as it is shown in Figure 1. Principally, it is basically distinguishing to consist of the initial boundary layer, separated free shear layer, reattachment zone, primary recirculation or separation region, corner eddy, redeveloping boundary layer and the second separation region. The dynamics of primary flow separation could be described as it flows. The state of the initial boundary layer determine the development of the separated free shear layer, being laminar, transitional, or turbulent flow. The unstable shear layer carries large vertical structures that split at the reattachment zone, a substantial portion of the flow is reversed upstream and supplies the recirculation stream. The primary recirculation region is revealed by recirculating vortices and flow reversal. Likewise, a small low velocity counter-rotating corner eddy, just behind the step, is formed due to the strong recirculation flow.

Nomenclature

Re	Reynolds number
h	Height
y	Length in y dimension
l	Length
U	Velocity
v	Kinematic Viscosity
P	Pressure
J	Mass Flux
k	Conductance
R	Reaction Rate
G	Gas
B	Bulk
S	Site
$\dot{m}_{dep}$	Mass deposition rate
$k_{f,r}$	Forward Arrhenius reaction rate
$k_{b,r}$	Backward Arrhenius reaction rate

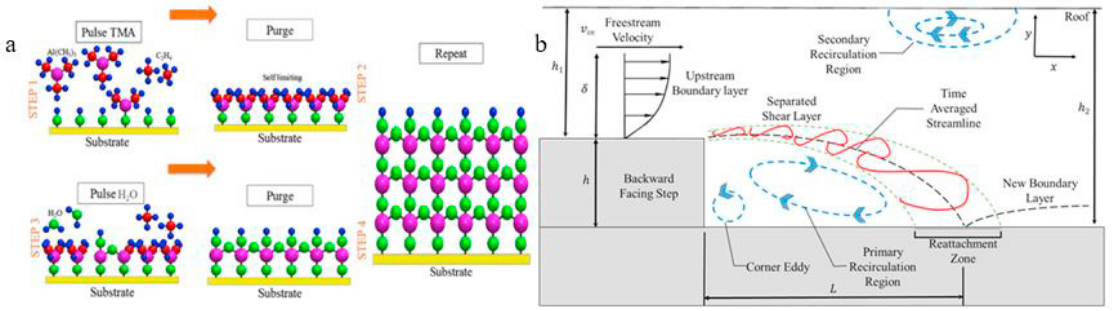

Fig. 1. (a) The ALD process; (b) The Detailed flow features of the Backward facing step flow (Authors own Illustrations)

The flow reattaches at a distance L from the step, and the new boundary layer develops, this is called the primary reattachment length, however, the recovery process is rather slow and the large-scale flow structures remain for a long distance downstream. This effect within the ALD reactor deposition process is of interest in this work.

The step height Reynolds number (Re_h) is defined as $Re_h = U_{max} h / \nu$, where U_{max} is the maximum inlet velocity, h is the step height, and ν the kinematic viscosity regarding the pulsating precursor/purge substance. The laminar regime follows for Re_h<900, whereas transitional regime is between Re_h>900 to Re_h<4950 and turbulent regime after Re_h>4950 [8]. Another parameter namely, the expansion ratio E, is defined as the ratio of the outlet channel height h_2 to the inlet channel height before the step h_1. these two prior parameters is a function of the primary reattachment distance L. Additionally to the primary recirculation region, a secondary recirculation region has been detected to exist within the laminar regime at Re_h>300 in the locale close to the roof. The location of the primary recirculation region could be significant in mass transfer, heat-transfer and chemical kinetic processes at the substrate wall. This may influence the deposition and growth of the ultrathin film. As such this study reports on the effect the flow field, near the substrate, due to change of step height at the manifold inlets, have on the ALD process deposition rate and growth uniformity.

2. Simulation Environment

2.1. The ALD Reactor Domain

The top half of a typical Gemstar 6 reactors, having a volume to surface area ratio off 883.18 cm^3/1585.54 cm^2, are simulated having two four port inlet manifolds. The ALD procedure injects trimethylaluminium (TMA), the first precursor, and ozone (O_3), the second precursor, sequentially after purging steps, into the reactor domain through inlet manifold 1 and inlet manifold 2, respectively, at 1.6 m/s for 0.2 sec. Between each precursor step, both inlet manifolds inject Argon inert-gas to purge the excess and by-products out of the system at 3.2 m/s for 5 sec. Initially, it is assumed that the first pulse will be exposed to a substrate that fully covered by oxygen (O) layer. The outlet and operating pressure is set to 1 torr. The substrate and reactor walls are heated to 200°C while the inlets are kept at 150°C. A step height (h) of 2.5mm, 5 mm, and 7.5mm, respectively, with an inlet diameter (D) of 5 mm and initial pre-step length (l_i) of 5 mm is observed in a 20 mm high roof to floor reactors. The inlet manifold is 23.5mm away from the wall boundary (y_1) with a pitch to pitch (y_2) and to symmetry length (y_3) of 18 mm. The Gemstar 6 reactors with the step height designs are shown in figure 2.

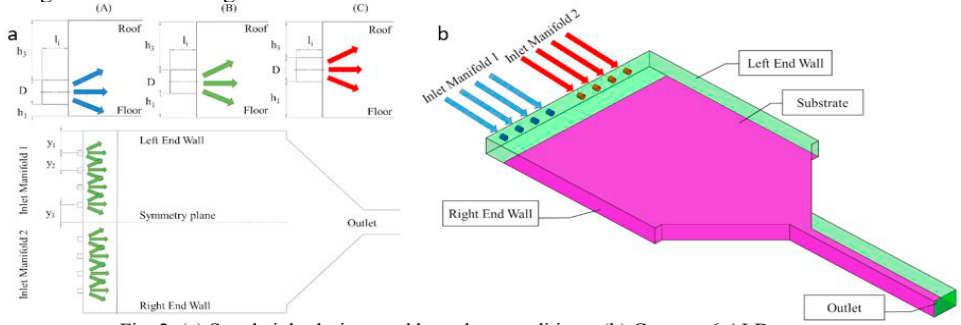

Fig. 2. (a) Step height designs and boundary conditions; (b) Gemstar 6 ALD reactor.

The deposition process of Al_2O_3 thin film surface reaction involves multiple reactive intermediates and elementary reactions, making it quite complex to simulate. As such, to simulate the chemical design problem the chemistry mechanism created by ChemkinPro is utilized along with ANSYS Fluent. The formulation and properties are similar to previous literature [2]. The reactors flow domains are meshed into 129 210, 134 208 and 134 881 nodes for the 5 mm, 7.5 mm, and 10 mm, respectively. The ALD process is numerically simulated applying the finite volume approach. Second order upwind and first order implicit methods is selected to discretize spatially and temporally, respectively. The pressure-velocity components are determined by the robust coupled algorithm solver. The transport equations source terms are linearized. Solution residuals are monitored and considered converged when less than $1x10^{-5}$ for the continuity, velocity and temperature components, and less than $1x10^{-4}$ for the species. Intrinsically, to simulate at a time step of $5x10^{-5}$ seconds a user defined function (UDF) is created to control the sequential ALD process. A similar process is used within Coetzee and Jen [12] previous works.

2.2. Mathematical Model

Modelling the ALD process consists of decoupling the physical and chemical processes first. The physical processes consisting of the governing laws of the conservation of mass, momentum transport, convective heat transfer, and species transport. These are decoupled from the chemical reactions. These governing laws are derived by corresponding partial differential equations (PDEs) that are solved numerically on the mesh domains defined nodes. Then, the PDEs are coupled to attain the completeness of the ALD numerical solution. This is obtained by considering the interactions between each physical and chemical process. The governing equations are stated as:

$$\frac{\partial \rho}{\partial t} + \nabla(\rho \overset{\mathrm{r}}{u}) = S_m \tag{1}$$

$$\frac{\partial \rho \vec{v}}{\partial t} + \nabla(\rho \vec{u}\vec{u}) = -\nabla P + \nabla \tau + \rho \vec{g} + \vec{F} \tag{2}$$

$$\frac{\partial \rho E}{\partial t} + \nabla\left(\overset{\mathrm{r}}{u}(\rho E + \rho\right) = \nabla\left(k_{eff} \nabla T - \sum h_i J_i\right) + R_r \tag{3}$$

$$\frac{\partial (\rho Y_i)}{\partial t} + \nabla \rho \vec{u} Y_i = -\nabla \vec{J_i} + R_i \tag{4}$$

The surface reactions with species transport are coupled by utilizing the laminar finite-rate method. The molar reaction rate for the irreversible surface reaction and the r^{th} irreversible surface reaction can be shown as:

$$R_r = k_{f,r}\left(\prod_{i=1}^{N_g} [C_i]_{wall}^{\eta_{i,gr}^{'}}\right)\left(\prod_{i=1}^{N_s} [S_j]_{wall}^{\eta_{i,sr}^{'}}\right) - k_{b,r}\left(\prod_{i=1}^{N_g} [C_i]_{wall}^{\eta_{i,gr}^{"}}\right)\left(\prod_{i=1}^{N_s} [S_j]_{wall}^{\eta_{i,sr}^{"}}\right) \tag{5}$$

$$\sum_{i=1}^{N_g} g_{i,r}^{'} G_i + \sum_{i=1}^{N_b} b_{i,r}^{'} B_i + \sum_{i=1}^{N_s} s_{i,r}^{'} S_i = \sum_{i=1}^{N_g} g_{i,r}^{"} G_i + \sum_{i=1}^{N_b} b_{i,r}^{"} B_i + \sum_{i=1}^{N_s} s_{i,r}^{"} S_i \tag{6}$$

Where G, B and S resemble the gaseous species, the bulk species, and the site species, respectively. The mass deposition rate ($\dot{m}_{dep}$) and wall shear (τ_x) at the substrate surface are expressed as:

$$\dot{m}_{dep} = \sum_{i=1}^{N_b} M_{w,i} \hat{R}_{i,bulk} \tag{7}$$

$$\tau_x = \mu(\partial u / \partial x) \tag{8}$$

3. Results and Discussion

Figure 3 reveals the three inlet step heights streamline flow behavior at the ozone and argon manifold. Within this section view the wall corners, as well as, the new boundary layer development near the substrate is shown. It is seen that the top step corner in this dual BFS phenomena, that a primary recirculation region is created regarding the Ozone and argon sequences. Contrary, the lower corner step reveals that only that the recirculation zone is present with a higher step dimension. However, it can then also be premised that a low velocity eddy corner is present in both steps. An interesting phenomenon is the magnitude the new boundary is formed within the lower step heights. The new boundary layer is fed with a higher force due to the substances impacting the floor and then reflected away. The smaller the step height the more impactful this phenomenon. In figure 4 (a), the ALD sequence substances to obtain the dimensional coordinates of the reattachment zones is analyzed between the wall shear and the x coordinate. Here the x coordinate is recorded from the bottom edge corner of the step (at -142.5 mm) until the midpoint of the reactor. The wall shear along the flow across the floor peaks with a higher velocity impacting the floor. The higher the step dimension, the slower the velocity impacting the floor as the flow slows down within the reactor. Although a slower velocity is then introduced to form the new boundary layer along the depositing substrate, this phenomenon may contribute to a more uniform film growth of the precursor substance. The 2.5mm step revealed the highest wall shear among its sequences, illustrating minimal to no recirculation regions, and allowing a higher velocity of flow to cover the substrate. This in turn respond with the highest deposition rate, as illustrated in figure 4 (b), and the average growth rate of 0.823 Å/cycle, 0.673 Å/cycle, and 0.579 Å/cycle for the 2.5, 5, 7.5 mm steps, respectively. These values, although bit low, is still within the margin to that of previous literature [13]. Argon flow is illustrated in figure 4 (a) as having the highest wall shear near the corner and along the substrate in all the step heights, respectively, since it is supplied at a higher velocity than that of the precursors.

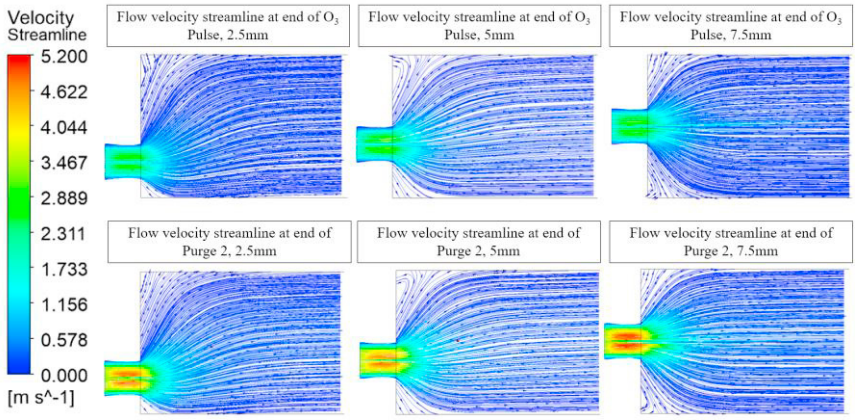

Fig. 3. (a) The streamline flow of a 2.5 mm step; (b) a 5 mm step; (c) and a 7.5mm step.

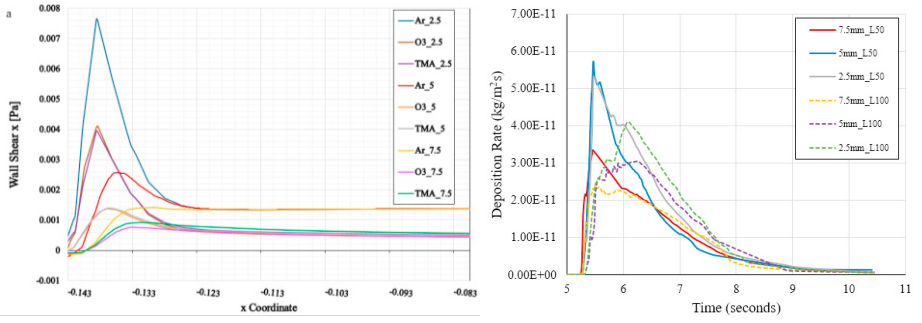

Fig. 4. (a) The precursor and purging substance wall shear along the floor; (b) the substrate midpoint deposition rate due to step height.

However, the precursor and purging sequences reveal similar wall shear along the substrate after the new boundary layer have been stabilized. This stabilization is favorable for ALD deposition as even and conformal growth can be more easily controlled along the substrate. The negative value of the wall shear exemplifies the recirculation flow presence in that specific ALD sequence.

Figure 4 (b) illustrates that the deposition rate regarding step heights away from the substrate. Within this illustration 50 mm and 100 mm was recorded in line with the Ozone precursor manifold. The higher the step height the lower the expected deposition rate. This can be explained as the velocity and vice versa the amount of precursor substances at the reactive site is reduced due to the new boundary layer being created with less force. It can also be mentioned that some of the precursors are subjected to the primary recirculation regions in both top and bottom step, reducing the amount of availability.

4. Conclusion

The BFS phenomenon does demonstrate to have an impact on the flow behavior along the substrate in a Gemstar 6 ALD reactor. The BFS explains the new velocity boundary creation after the reattachment zone and primary recirculation region development with the different step height. It is seen that the deposition rate is depended on the velocity and amount of substance along the substrate, and the flow velocity producing the reactive precursor to the substrate is influenced by the force that creates the new velocity boundary layer. This revealed a reduced deposition rate about an increasing step height. The step height regarding the inlet velocity creates recirculation zones along all ALD sequence substances, the wall shear is used to identify the recirculation flow and reattachment length. The author emphasizes the interest of the BFS phenomena in nanotechnology fabrication processes and motivates the continual study of the BFS phenomena, especially the velocity flow, mass, heat transfer and chemical reaction effects in the ALD process.

Acknowledgements

The authors would like to acknowledge the Global Excellence and Stature (GES) and National Research Foundation (NRF), South Africa for the financial support. Also, the University of Science and Technology of China (USTC) for providing the required design data and assistance in the research and CHPC for the computing resources.

References

[1] R.A. Wind, S.M. George, Quartz Crystal Microbalance Studies of Al_2O_3 Atomic Layer Deposition Using Trimethylaluminum and Water at 125 °C, The Journal of Physical Chemistry A, 114 (2010) 1281-1289.
[2] M.R. Shaeri, T.C. Jen, C.Y. Yuan, Reactor scale simulation of an atomic layer deposition process, Chemical Engineering Research and Design, 94 (2015) 584-593.
[3] G.P. Gakis, H. Vergnes, E. Scheid, C. Vahlas, B. Caussat, A.G. Boudouvis, Computational Fluid Dynamics simulation of the ALD of alumina from TMA and H2O in a commercial reactor, Chemical Engineering Research and Design, 132 (2018) 795-811.
[4] Z. Baji, Z. Lábadi, G. Molnár, B. Pécz, K. Vad, Z.E. Horváth, P.J. Szabó, T. Nagata, J. Volk, Highly conductive epitaxial ZnO layers deposited by atomic layer deposition, Thin Solid Films, 562 (2014) 485-489.
[5] J.W. Elam, S.M. George, Growth of ZnO/Al_2O_3 Alloy Films Using Atomic Layer Deposition Techniques, Chemistry of Materials, 15 (2003) 1020-1028.
[6] L. Huiling, B. Xiaobin, Z. Shengdong, Z. Hang, Ultraviolet detecting properties of amorphous MgInO thin film phototransistors, Semiconductor Science and Technology, 30 (2015) 125010.
[7] C. Gualtieri, Numerical Simulations of Laminar Backward-Facing Step Flow With FEMLAB 3.1, 2005 (2005) 657-662.
[8] B.F. Armaly, F. Durst, J.C.F. Pereira, B. Schönung, Experimental and theoretical investigation of backward-facing step flow, Journal of Fluid Mechanics, 127 (2006) 473-496.
[9] R. Mittal, U. Madanan, R.J. Goldstein, The heat/mass transfer analogy for a backward facing step, International Journal of Heat and Mass Transfer, 113 (2017) 411-422.
[10] M. Shahi, J.B.W. Kok, A. Pozarlik, On characteristics of a non-reacting and a reacting turbulent flow over a backward facing step (BFS), International Communications in Heat and Mass Transfer, 61 (2015) 16-25.
[11] A.S. Kherbeet, H.A. Mohammed, K.M. Munisamy, B.H. Salman, The effect of step height of microscale backward-facing step on mixed convection nanofluid flow and heat transfer characteristics, International Journal of Heat and Mass Transfer, 68 (2014) 554-566.
[12] R.A.M. Coetzee, T.-C. Jen, The Mechanistic Process Comparison Between a Novel Slotted Injection Manifold Versus the Multiple Injection Manifold of a Low Pressure Square Type Atomic Layer Deposition Reactor, (2018) V002T002A039.
[13] D. Pan, D. Guan, T.-C. Jen, C. Yuan, Atomic Layer Deposition Process Modeling and Experimental Investigation for Sustainable Manufacturing of Nano Thin Films, Journal of Manufacturing Science and Engineering, 138 (2016).